Hindawi
International Journal of Geophysics
Volume 2023, Article ID 1209844, 10 pages
https://doi.org/10.1155/2023/1209844

Research Article

Rock Type Effects on Radio Signal Attenuation

Kai Kordelin,[1] **Johanna Virkki**,[1] **Jaana Kordelin**,[1] **Juhani Norokallio**,[2] **Jari Heikkinen**,[2] **Jyrki Liimatainen**,[2] **Leena Ukkonen**,[1] **and Lauri Sydänheimo**[1]

[1]*Faculty of Medicine and Health Technology, Tampere University, Finland*
[2]*Posiva (Finland), Eurajoki, Finland*

Correspondence should be addressed to Kai Kordelin; kai@kordelin.eu

Received 8 June 2022; Revised 16 January 2023; Accepted 18 January 2023; Published 1 February 2023

Academic Editor: Arkoprovo Biswas

This research work is aimed at studying different rock types and the effect of their mineral contents on an active 434 MHz RFID card's radio signal attenuation. This research was done at the ONKALO nuclear waste storage facility using radio frequency identification (RFID) equipment. First, the studied area and research plan, including the used system and equipment, are explained. After this, the researched areas of rock types and their effects on radio signals are presented. This work focused mainly on occupational safety, but it also investigated whether it would be possible to use RFID technology in producing mines as well, especially in the boundary layer of the ore body. This research can help the design of communication frequencies for autonomous devices.

1. Introduction

Today, companies are increasingly investing in occupational safety. From the point of view of occupational safety, it is important to know where people are working. Mines and other underground worksites have various solutions for monitoring persons. At first, Posiva used a so-called washer board (Figure 1). The washer board was used to know how many people there are in ONKALO. Each person working in the tunnel had a hook with their name on the washer board. On the hook, they put a washer every time they went to ONKALO and took it out when they left ONKALO [1]. The problem with the washer board is that it is based on worker activity. From the point of view of occupational safety, an automatic system independent of personal activities is safer.

Posiva Oy is an expert organization in environmental technology, established in 1995, and the leading final disposal operator in the world. Posiva is preparing to start 2020's final disposal of spent nuclear fuel in the ONKALO facility excavated deep in the bedrock. ONKALO's layout and study area are shown in Figure 2. Posiva is tasked with handling the final disposal of the spent nuclear fuel generated by its owners because Finnish law states that nuclear waste producers are responsible for all nuclear waste management measures and costs [2].

This research was done at the ONKALO nuclear waste final storage facility [2, 3]. In other studies, signal attenuation has been studied, and measurements have been made in different environments, concrete tunnels, coal mines with rock dust and shotcrete, with and without conductive mesh, and hard rock mines [4–6]. Our previous study studies the effects of bedrock-sprayed concrete mixture that includes stainless steel fibers on antenna reading areas. During this study, it was found that the minerals in the bedrock affected the reading areas [7].

Studies are being conducted to gain experience in the reliability of various systems. From the point of view of occupational safety, it is necessary to know what things can impair the readability of the system. This study is aimed at finding out how different rock types, their mineral contents, and grain size affect radio signal propagation. In the future, based on this gathered data, optimal antenna locations could be defined in the bedrock during the bedrock mapping phase. It would improve occupational safety. Occupational safety is always essential. However, it is even more vital to know who is in there in underground tunnels and mines, and this information must be extremely reliable.

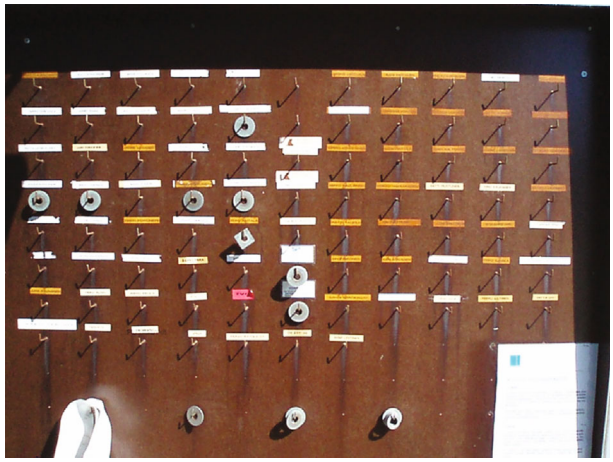

Figure 1: Washer board [1].

Also, companies can use this information for occupational safety in road and railway tunnel construction before spraying concrete during the construction phase. For companies doing productive mining, this information could help with cost savings. Cost savings occur, especially when mining near the ore body boundary layer.

This study was performed using a Wavetrend active RX201-system. The ID (identification) card is an active transmitting unit in this system, and the reader is only the receiving unit (Figure 3). The Wavetrend ID card is 85 mm long, 55 mm wide, and 5 mm thick sealed plastic casing that contains the electrical power source and an antenna. Each ID card is supplied with a unique ID number that the receiver system detects. The ID card transmits its unique ID number every 1.5 seconds at a frequency of 434 MHz [8]. All people and all vehicles have their ID cards [1].

In this study, RSSI (received signal strength indicator) values and susceptibility values were used as measurement values. According to the RX201 manual, the reader's RSSI can be adjusted between 60 and 120, where 60 is the weakest RSSI value. The RX201 sensitivity is -103 dBm, meaning RSSI 60 is equal to -103 dBm. No other dBm values are given, and thus, it is not possible to make a conversion chart between RSSI and received power [8].

Magnetic susceptibility interferes with the propagation of radio signals. Magnetic susceptibility K is defined by $M = [K] \times H$, where M is the induced magnetization of the material and H is the inducing magnetic field. As both M and H are expressed in amperes per meter, volumetric susceptibility K is a dimensionless "SI unit," while mass susceptibility $X = K/p$ is in cubic meters per kilogram [9–11]. A KAPPAMETER model KT-6 instrument by SatisGeo (Figure 4(b)) was used for the susceptibility measurements. The instrument's sensibility is 1×10^{-5} SI units, and the measurement range is -999 to 9999×10^{-3} SI units. The manufacturer of this meter is SatisGeo s.r.o. [12]. The susceptibility scale is logarithmic.

The area selected for this study was the ONKALO tunnel system's so-called Demo 3 in level –420 (Figure 2). Demo 3 is a 25-meter-long tunnel whose bedrock is not covered because it is desired to monitor geological changes in the tunnel even more than 100 years. In this way, the tunnel geological changes can also be monitored in the future. The lithology of the tunnel is versatile, which makes it ideal for studying radio signals [13–15].

2. Measurement Setup

The study protocol consists of four measurement sets. Measurement location choices were based on the composition of the rocks. The first and the second measurement sets had 17 measurement locations. The third measurement set had nine measurement locations, and the fourth measurement set had two measurement locations. The ID card was in the same position where employees held it in every measurement set. The study was conducted with Wavetrend's system because these devices are part of Posiva's occupational safety. The aim was to gain insight into situations where problems might arise in its operation.

In the first measurement set, the ID card was attached to the bedrock of different rock types, and then, the RSSI value was measured. In addition to this, the susceptibility value was also measured. The 17 locations of the measurement were selected and marked to photos taken during the geological mapping. Figure 4 demonstrates the measurements done at the Demo 3 tunnel. First, the RSSI and susceptibility values were measured from each location. Only one active ID card was used when measuring the RSSI values, so the ID card's differences would not affect the results. During these measurements, the ID card was attached to the bedrock. The susceptibility measurements were done from the same locations.

Susceptibility means the ratio of magnetization produced in a material to the magnetizing force [16]. Magnetic susceptibility, the ratio of induced magnetization to an applied magnetic field, is a function of strongly magnetic particle concentrations, grain sizes, grain shapes, and mineralogy [17]. Figure 5 demonstrates what susceptibility is. There are several theoretical studies of the progression of susceptibility and electromagnetic fields. However, most studies focus on homogenetic materials. As rock types are heterogenetic and their magnetic structure is complicated, this theoretical knowledge is difficult to apply [17, 18]. Rock cannot be magnetized in a solid state. Magnetization can only happen when rock is in a molten state. The change in magnetism has occurred more than 1300 million years ago [19]. This study does not take a position on what kind of type magnetism the bedrock material is. In the study area, the strength of the magnetic field of the bedrock is so weak that it does not significantly affect the receiver.

In the second measurement set, the difference in RSSI value was measured when the ID card was attached to the bedrock and then detached 50 mm from the bedrock surface. The purpose of the second measurement set was to confirm the reliability of the RSSI value of the first measurement set. The measurements were done at the same locations as the first measurement. First, the active ID card was against the bedrock, and then, the ID card was about 50 mm off the bedrock. This was to see how much the RSSI value changes once

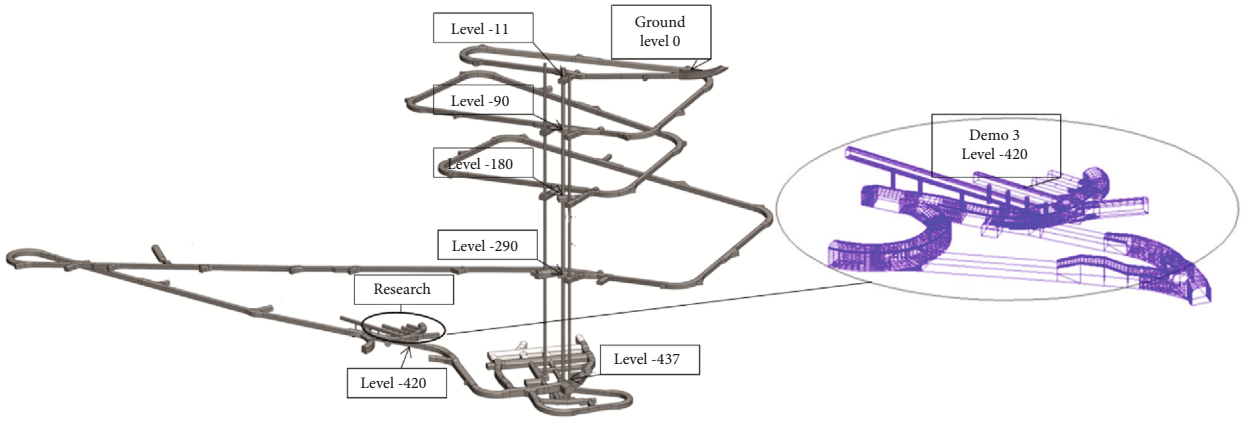

Figure 2: Study area at the ONKALO tunnel system.

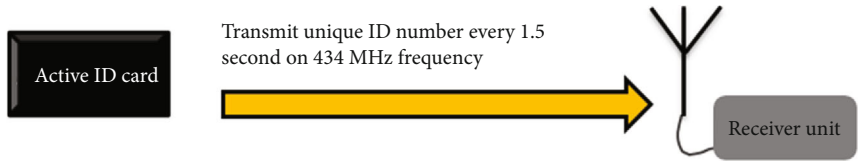

Figure 3: Active ID card transmits a unique ID number to the receiver unit.

(a)

(b) (c)

Figure 4: View of the measurement (a), susceptibility measurement (b), and RSSI value measurement (c).

the card is not touching the bedrock. This measurement was carried out with four ID cards to see if differences in each ID card affected the RSSI value.

The third measurement set was made because the advisor board suggested that an external surveyor makes the measurements. These procedure suds increase the reliability of the measurements. An external research assistant selected random locations in this measurement set. After this, the geologist reported the rock types, grain size, and amount of minerals at measurement locations.

The fourth measurement set was also done in Demo 3. After the initial measurement sets, it was possible to measure two different rock types. The measurement results are good to know from the view of occupational safety. One measurement was done from a rock sample found in an inclusion (inclusion means, in geology, a body or particle of distinct composition embedded in a rock or other material) at ONKALO's parking area. This specimen differs entirely from the rock type in the Demo 3 area and the Olkiluoto area lithology. Another measurement was done using a rock sample from the Kemi chrome mine [21]. Both examples differ entirely from the rock type used for the initial measurements. It was interesting to find out how a completely different type of rock affected the RSSI value.

3. Rock Types at Measurement Locations

In the following, the Olkiluoto rock types, resistivity range, and the measurement location's rock types, grain sizes, and minerals are explained in general.

The bedrock of Olkiluoto consists mainly of migmatites, i.e., they are mixtures of different rock types. Migmatites commonly show clear striping. Lighter and darker rock types alternate in different thickness layers (Figures 6–8). The grain size of the rock varies. The grain size is divided into four groups: fine-grained (<1 mm), medium-grained (1-5 mm), coarse-grained (5-50 mm), and large-grained (>50 mm).

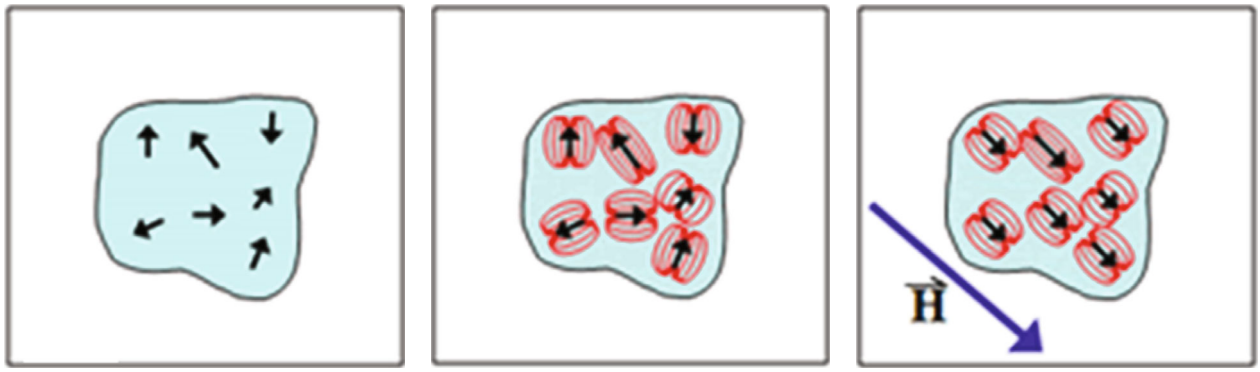

Figure 5: (a) No external field, and the rock sample has zero net field. (b) Magnetic domains are oriented randomly. (c) If an external field H exists, magnetic domains will align to it [20].

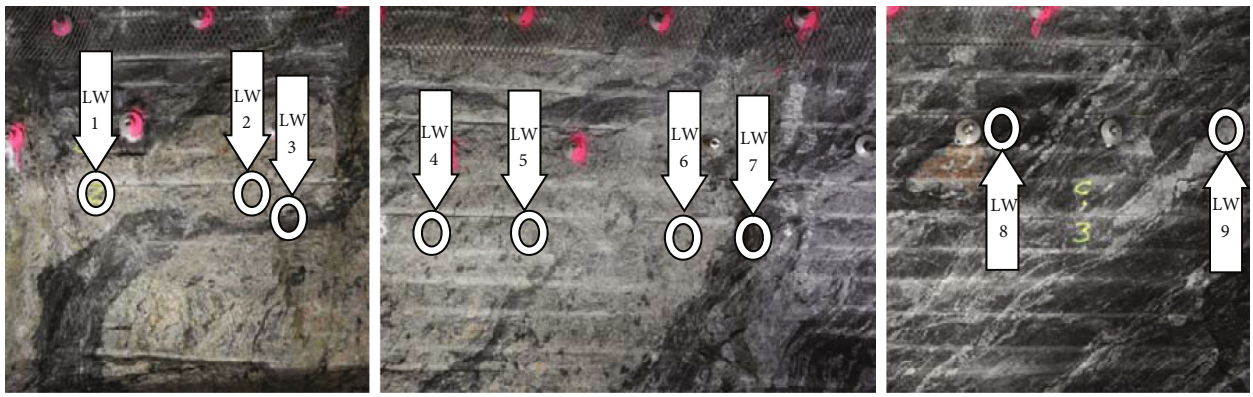

Figure 6: Demo 3 left wall.

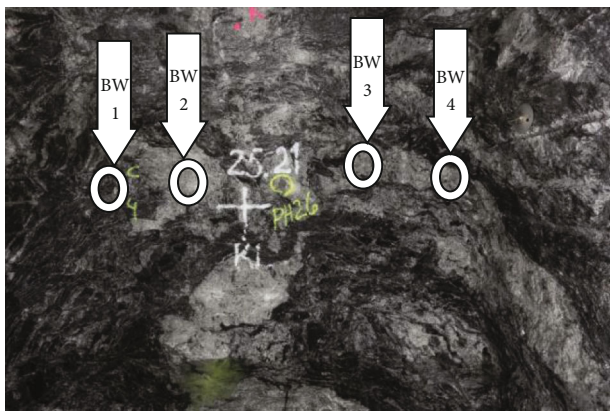

Figure 7: Demo 3 back wall.

The resistivity measurements have been made in ONKALO from rock samples taken between 2005 and 2008. Resistivity measurements used three frequencies, 0.1 Hz, 10 Hz, and 50 Hz, which have also been used to compute the frequency effect of induced polarization (IP value). Values are slightly dispersive, i.e., decreasing with increasing frequency [21].

Conductivity is contributed by rock constituents of metallic conductors, nonconductors, insulators, semiconductors, and electrolytes. Most rock-forming minerals are semiconductors (oxides and sulfides, of weak to moderate conductivity) or insulators (most silicates, of high resistivity). Rock mass resistivity is formed as a mixture of these components, will express similar behavior under dry conditions, and has a very high range of variation from 10^{-8} to $10^{17}\,\Omega$m [22].

Most of the electrical conductivity contribution is created or enhanced by the electrolyte in pore space and fractures. Resistivity is considered a rather indicative parameter of lithology in sedimentary rocks (defined as grain size and, e.g., clay content). It will correlate strongly with porosity and texture in metamorphic rocks. Resistivity decreases with increasing pore space and fracturing. Accessory semiconductor minerals (graphite and sulfides) will decrease resistivity [23].

The lighter bands and areas are mainly pegmatitic granite, which is coarse- and large-grained. The mica amount, especially dark biotite (biotite is a mineral in the mica group), is small, but quartz and feldspar quantities are high. The darker bands in the rock are very mica-rich, and the grain size is typically medium-grained. The darker areas can also contain fine-grained and quartz-rich areas [13–15, 24, 25]. In Table 1, the Olkiluoto bedrock stone species are shown with their resistivity range [22]. In this

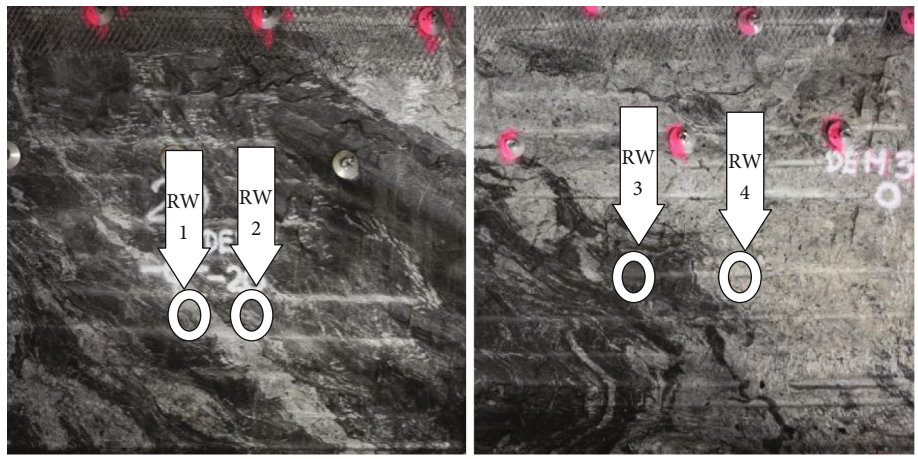

Figure 8: Demo 3 right wall.

study, the most common rock types are on the top and descending to the bottom.

The resistivity distribution of PGR (pegmatitic granite) is very close to the resistivity distribution of all the samples. However, PGR has only a few highest resistivity values (>50000 Ωm). Therefore, its median resistivity is lower than the median of all the values. Resistivity distributions of VGN (veined gneiss) and MGN (mica gneiss) are very close to the resistivity distribution of all the samples. TGG (tonalitic granitic granodioritic gneiss) has the highest resistivity of all the samples. QGN (quartz gneiss) has a very high resistivity as well [22].

In the first measurement set, the aim was to select the measurement locations in such a way that they give the most representative samples. These 17 locations were marked on the photos taken during the geological mapping. Figures 6–8 also show the locations where the Posiva leading geologist had reported the measurement of rock type, grain size, and mineral amount.

Figure 6 shows the left-side measurement locations of the Demo 3 area. The rock types and structure of the measurement location are given.

(i) LW 1: coarse- and large-grained PGR

(ii) LW 2: coarse-grained PGR

(iii) LW 3: medium- and fine-grained QGN that also consists of some dark biotite

(iv) LW 4: coarse- and large-grained PGR

(v) LW 5: coarse- and large-grained PGR

(vi) LW 6: coarse-grained PGR

(vii) LW 7: coarse-grained biotite-rich area and mica gneiss MGN

(viii) LW 8: fine-grained quartz-gneiss QGN, but next to this point also biotite-rich mica gneiss MGN

(ix) LW 9: medium- and coarse-grained PGR

Figure 7 shows the rear measurement locations of the Demo 3 area. The rock types and structure of the measurement location are given.

(i) BW 1: medium-grained biotite-rich mica gneiss MGN

(ii) BW 2: medium-coarse-grained PGR

(iii) BW 3: inside PGR biotite-rich area

(iv) BW 4: coarse-grained PGR

Figure 8 shows the right-side measurement locations of the Demo 3 area. The rock types and structure of the measurement location are given.

(i) RW 1: coarse-grained and quartz-rich PGR

(ii) RW 2: medium-grained mica-rich dark band and in the same area medium-grained, fine-grained mica- and quartz-rich area

(iii) RW 3: medium-grained and fine-grained mica- and quartz-rich area edges contain some biotite-rich mica gneiss

(iv) RW 4: coarse- and large-grained PGR and quartz-rich area

The third measurement set locations have not been marked in pictures. The third measurement set had nine measurement locations, of which eight measurement locations contained the same rock types as the first and the second measurement sets. Only one measurement location differed significantly from the first and the second measurement sets. This rock was fine- to medium-grained VGN (veined gneiss) that contained a mica-rich band.

The reason why the fourth measurement set was done was occupational safety. Sample 1 is a rock originating from an inclusion found inside a VGN. The rock is very mineral-rich and consists of quartz, plagioclase, chlorite,

Table 1: Resistivity ranges for the different rock types [21].

	Rock type	Resistivity median (Ωm)	Resistivity min (Ωm)	Resistivity max (Ωm)	Mode(s) (Ωm)	Range(s) (Ωm)	Std. dev (Ωm)
VGN	Veined gneiss	22800.00	20	2042772	2-3 k 6-8 k 20-25 k 60-100 k 250 k	4-40 k 60-100 k	151097
PGR	Pegmatitic granite	16300.00	188	472170	6-8 k 16-20 k 25-30 k	3-30 k	145948
DGN	Diatextic granite	15500.00	9.46	942538	3-4 k 4-5 k 10-12 k 20-25 k 40-50 k	5-65 k	106169
SGN	Stromatic gneiss	18800.00	2459	623413			
MGN	Mica gneiss	20400.00	358	666192	4-5 k 20-25 k 60-100 k	3-30 k 60-200 k	110824
QGN	Quartz gneiss	55800.00	10600	475925	10-15 k 20-160 k 250-320 k	10-500 k	183258
KFP	K-feldspar porphyry	5730.00	3500	30300			
MFGN	Mafic gneiss	18900.00	534	465740	1-1,5 k 6-10 k 20-100 k	6-100 k	108686
TGG	Tonalitic granitic Granodioritic gneiss	24400.00	2190	460063	10-12 k 20-32 k	6-40 k	102174
MDB	Metadiabase	113000.00	16200	463038			
All		19366.50	9.46	2042772	6-8 k 16-32 k	4-100 k	118614
Altered		12386.50	9.46	2042772	2-3 k 5-6 k 10-12 k 25-32 k 40-50 k	5-50 k	143048
Deformed					1-2 k 5-6 k	4-30 k	88168

and pyrrhotite. Also, a rock core sample 2 received from the Kemi chrome mine was measured. The rock sample consists of chromitite, and its main mineral is the chromite.

4. Measurement Results

Table 2 shows the results of the first measurement set and second measurement set. These 17 measurement locations are shown in Figures 6–8. The table illustrates the connection between RSSI value and susceptibility. The reference RSSI value shown in the table has been measured in the middle of the tunnel, approximately four meters from the reader antenna, which only acts as a receiver.

Figure 9 shows the RSSI and the susceptibility values of the first measurement set as a histogram. You can also see the average of the RSSI and susceptibility values. Circles have marked the points where the susceptibility values exceed the average. Figure 9 shows when the susceptibility value grows and the RSSI value decreases.

Table 3 shows the results of the third measurement set and fourth measurement set RSSI values. One italic result in Table 3 shows that in the third measurement set, only one measurement location contained a different rock type than the first and second measurement sets.

Table 4 shows the results of the second measurement set, the third measurement set, and the fourth additional measurement set results. Table 4 contains the measurement

Table 2: Measurement location rock types, RSSI, and susceptibility value.

Measure point	Tag ID	First measurement set		Second measurement set						
	Rock type	Susceptibility	1224 RSSI value	1232 RSSI on bedrock	1232 RSSI 50 mm off bedrock	1233 RSSI on bedrock	1233 RSSI 50 mm off bedrock	1234 RSSI on bedrock	1234 RSSI 50 mm off bedrock	1235 RSSI on bedrock	1235 RSSI 50 mm off bedrock
LW 1	PGR	0.03	135	135	134	134	134	135	135	134	135
LW 2	PGR	0.05	131	131	130	131	131	131	131	130	131
LW 3	QGN	0.15	126	123	126	124	127	126	127	126	126
LW 4	PGR	0.05	130	130	131	129	130	130	130	129	130
LW 5	PGR	0.04	132	132	133	134	135	133	134	132	132
LW 6	PGR	0.04	129	129	129	127	128	129	130	130	131
LW 7	Biotite-rich MGN	0.25	99	99	111	100	108	99	106	98	107
LW 8	QGN+biotite-rich MGN	0.15	120	120	126	118	122	119	124	120	124
LW 9	PGR	0.03	125	125	124	126	126	125	126	125	126
BW 1	Biotite+MGN	0.27	111	111	125	110	128	111	128	111	126
BW 2	PGR	0.07	122	122	122	120	121	122	123	122	122
BW 3	Biotite	0.19	116	116	126	114	126	114	127	116	132
BW 4	PGR	0.05	125	125	125	125	125	125	125	125	125
RW 1	PGR	0.04	111	111	110	111	112	110	110	112	112
RW 2	Mica-rich	0.22	94	93	106	93	108	96	111	94	109
RW 3	Mica-rich	0.33	93	93	107	94	110	95	110	93	107
RW 4	PGR	0.07	116	116	115	116	117	115	116	116	116
Reference value		0	135								

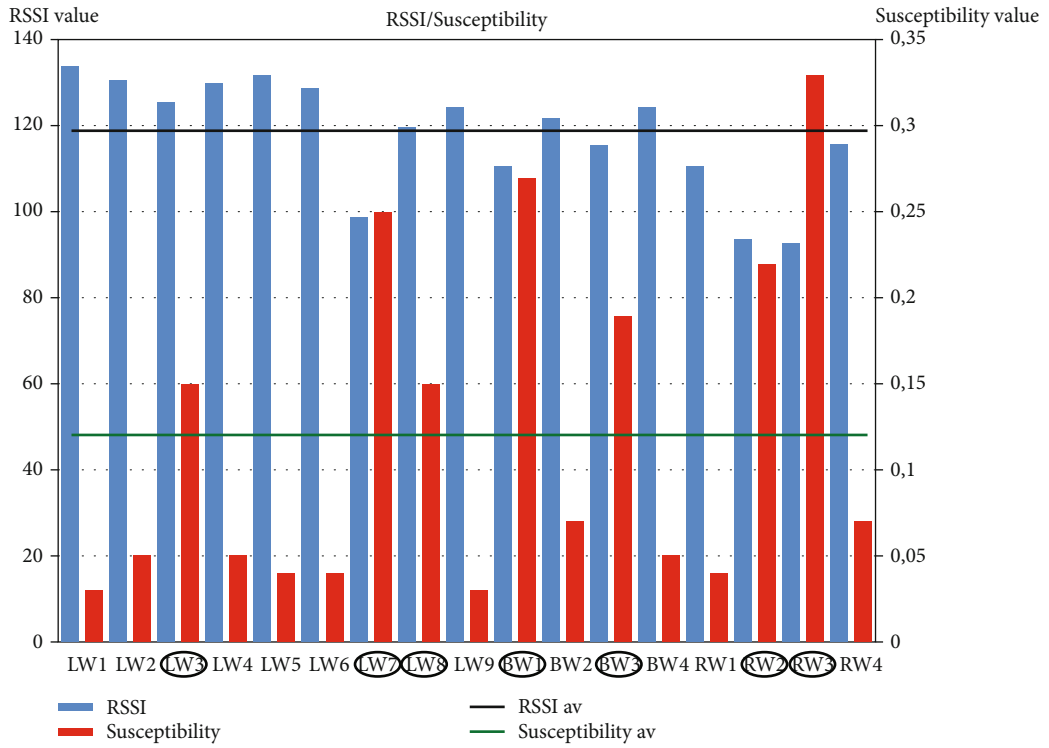

Figure 9: Measured RSSI and susceptibility values and their averages.

Table 3: The third measurement set and the fourth measurement set rock types and RSSI value.

(a)

	Third measurement set	
	RSSI	Rock type
Location 1	134	PGR
Location 2	127	QGN
Location 3	100	Biotite-rich MGN
Location 4	132	PGR
Location 5	130	PGR
Location 6	**122**	*VGN - mica-rich*
Location 7	126	PGR
Location 8	117	Biotite
Location 9	120	QGN+biotite-rich MGN

(b)

	Fourth measurement set	
	RSSI	Rock type
Sample 1	105-120	VGN+quartz+plagioclase+chlorite +pyrrhotite
Sample 2	75-90	Chromitite

results by rock type. Table 4 shows the change of RSSI value in different rock types when the ID card is on the bedrock and then 50 mm of the bedrock.

Table 4: RSSI value changes by rock types.

Rock type	Change of RSSI value
PGR	±1
QGN	+1–+4
Biotite-rich MGN	+6–+12
QGN+biotite-rich MGN	+2–+6
Mica-rich	+10–+15
Biotite+MGN	+12–+18
Biotite	+10–+16
VGN+mica-rich	+6–+10
VGN+quartz+plagioclase+chlorite+pyrrhotite	+15–+30
Chromitite	+40–+60

5. IAEA Measurements in This Research Area

Investigation of the GPR (*g*round-*p*enetrating *r*adar) technique uses electromagnetic radiation pulses in the radio spectrum's microwave band (10 MHz to 3 GHz). It reads the reflected signal to detect subsurface structures and objects without drilling, probing, or otherwise breaking the ground surface. GPR uses transmitting and receiving antennae. The transmitting antenna radiates short pulses of high-frequency radio waves into the ground. When the wave hits a buried object or a boundary with different electrical properties, the receiving antenna records variations in the reflected return signal. Using the time differences in the reflected waves, it is possible to reconstruct images of

subsurface structure and look for voids, cracks, or other inhomogeneities [26].

GPR has been used by the IAEA (International Atomic Energy Agency) since 2006 for design information verification and inspection of concrete during the construction of new nuclear facilities but has never been used in a GR (ground radar) on a bare rock before [26].

GPR signal attenuation is challenging in the Finnish bedrock, which is a mix of pegmatitic and gneissic rock. Rock type, fracture zones, fracture intensity, fracture fillings, and water content strongly affect signal attenuation. Generally, the high conductivity and high dielectric value (permittivity) of the medium (rock) strongly attenuate the GPR signal [26].

Geovisor executed low-frequency ground-penetrating radar measurements in ONKALO for IAEA. The main goal of the measurements was to carry out GSSI's (Geophysical Survey Systems Inc.) GPR equipment feasibility test in detecting voids in ONKALO rock conditions. The campaign consisted of measurements with four low-frequency antennas 100, 270, 350, and 400 MHz [26].

As assumed, the very low-frequency antennas (100 and 270 MHz) do not work ideally in tunnel conditions. Large dimensions of antennas, very low frequencies, intensive ringing effect, and old technology are the weaknesses of these antennas. Based on the testing, 350 MHz and 400 MHz are the most suitable antennas for ONKALO rock and overall tunnel conditions [26].

6. Analysis of Measurements

6.1. Susceptibility Effect and RSSI Value. Without question, the first measurement set indicated the mineral's effect on the RSSI values. Table 2, together with Figure 9, provides a good illustration of how mica and minerals weaken the RSSI value and increase the susceptibility compared to PGR, which does not contain mica. The grain size of the rock did not have any effect on the RSSI value or the susceptibility. Figure 9 circles those points when the susceptibility is above average, and the RSSI value is low.

6.2. Mineral Effect and RSSI Value. The second, third, and fourth measurement sets confirmed the first measurement set results. The results of Tables 4 and 2show that rock types strongly affect RSSI values. The ID card RSSI value change on the bedrock to 50 mm off the bedrock varied according to rock types.

In the first and second measurement sets, when the rock type was PGR, the RSSI value did not change.

(i) When the rock type was QGN, the RSSI value change was 1-4 units

(ii) When the rock type was biotite-rich MGN, the RSSI value change was 6-12 units

(iii) When the rock type was QGN+biotite-rich MGN, the RSSI value change was 2-6 units

(iv) When the rock types were mica- and quartz-rich (mica-rich, biotite+MGN, and biotite), the RSSI value change was up to 18 units

In the third measurement set, one measurement location contained a different rock type than the first measurement set. This rock type was fine to moderately grained VGN veined gneiss that contained a mica-rich band. In this location, the RSSI value change was 6-10 units.

The fourth measurement set was done with a rock that originates from an inclusion found inside a VGN. The rock is mineral-rich and consists of quartz, plagioclase, chlorite, and pyrrhotite. These minerals weakened the ID card's RSSI value by up to 30 units. The most significant measured differences in values were recorded when measuring a rock core sample from the Kemi mine. This rock sample consists of chromitite, and its main mineral is chromite. This rock specimen measurement changed the RSSI value by up to 60 units.

6.3. Analysis of Measurements. The IAEA measurements give the same kind of conclusion as our measurements. The bedrock of ONKALO absorbs low-frequency radio waves. The absorption of radio frequencies must also be considered if autonomous means of transport are to be used in the final disposal of nuclear waste.

7. Conclusion

This research provides an understanding of how different rock types and minerals within them affect the RSSI values at 434 MHz. Based on this research, the grain size of the rock type did not affect the RSSI value, but the type of rock and its mineral content had an effect. The mineral's magnetism had a strong impact. The higher the susceptibility value was, the lower the RSSI value correspondingly was. Future measurements should be performed with different radio frequencies. This would further help us understand how different radio frequencies react with different rock types and minerals contained within.

These results will help occupational safety by better determining where to locate antennas. The antenna should not be placed in an area containing a lot of mica and quartz, as they both decrease the reading reliability. However, from the point of view of occupational safety, it is good to note that when the ID card is off the bedrock, the RSSI value increases fast. This provides reliable information on employees existing in tunnels and increases occupational safety.

This research also supports the theory that it is possible to detect minerals in rocks using radio waves. Results could be used in the mining industry with production quarries.

The change caused by chromitite was so significant that it must be considered for occupational safety in production mines.

Data Availability

The xlsx data used to support the findings of this study are available from the corresponding author upon request.

Conflicts of Interest

The authors declare that they have no conflicts of interest.

References

[1] K. Kordelin, J. Kordelin, J. Virkki, M. Johansson, L. Ukkonen, and L. Sydänheimo, "Development and implementation of an RFID-based tunnel access monitoring systems," *Science and Technology of Nuclear Installations*, vol. 2016, Article ID 9897675, 10 pages, 2016.

[2] P. Oyhttp://posiva.fi/en.

[3] T. Saanio, A. Ikonen, P. Keto et al., "Design of the disposal facility 2012," *Working Report 2013-17*, Posiva Oy, Eurajoki, 2013, http://www.iaea.org/inis/collection/NCLCollectionStore/_Public/45/087/45087772.pdf.

[4] C. Zhou, T. Plass, R. Jacksha, and J. A. Waynert, "RF propagation in mines and tunnels: extensive measurements for vertically, horizontally, and cross-polarized signals in mines and tunnels," *IEEE Antennas and Propagation Magazine*, vol. 57, no. 4, pp. 88–102, 2015.

[5] M. Boutin, A. Benzakour, C. Despins, and S. Affes, "Radio wave characterization and modeling in underground mine tunnels," *IEEE Transactions on Antennas and Propagation*, vol. 56, no. 2, pp. 540–549, 2008.

[6] R. Jacksha and C. Zhou, "Measurement of RF propagation around corners in underground mines and tunnels," *Transactions*, vol. 340, no. 1, pp. 30–37, 2016.

[7] K. Kordelin, J. Kordelin, J. Virkki et al., "Optimization of RFID-based tunnel access monitoring system antenna reading areas," in *13th European Conference on Antennas and Propagation (EuCAP)*, pp. 1–5, Krakow, Poland, 2019.

[8] K. Kordelin, J. Kordelin, J. Virkki, M. Johansson, L. Ukkonen, and L. Sydänheimo, "Experimental study on RFID antenna reading areas in a tunnel system," *Journal of Engineering*, vol. 2017, Article ID 3850835, 15 pages, 2017.

[9] P. Rochette, M. Jackson, and C. Aubourg, "Rock magnetism and the interpretation of anisotropy of magnetic susceptibility," *Available in Reviews of Geophysics*, vol. 30, no. 3, pp. 209–226, 1992.

[10] L. Tauxe, S. K. Banerjee, R. F. Butler, and R. van der Voo, *Essentials of Paleomagnetism*, University of California Press, 5th edition, 2018.

[11] "Magnetic susceptibility. Available online: Magnetic susceptibility - Wikipedia," https://en.wikipedia.org/wiki/Magnetic_susceptibility.

[12] "SatisGeo - Instruments for geophysics and environment," https://satisgeo.com.

[13] N. Nordbäck, "Outcome of the geological mapping of the onkalo underground research facility, chainage 3116-4986," *Working Report 2013-11*, Posiva Oy, Eurajoki, 2013, http://www.posiva.fi/files/3089/WR_2013-11.pdf.

[14] E. Heikkinen, P. Kantia, T. Lehtimäki, M. Silvast, and B. Wiljanen, "EDZ assessments in various geological environments using GPR method," *Working Report 2010-04*, Posiva Oy, Eurajoki, 2010, http://www.posiva.fi/files/1311/WR_2010-04web.pdf.

[15] J. Norokallio, "Geological and geotechnical mapping procedures in use in the onkalo," *Posiva Report 2015-01*, Posiva Oy, Eurajoki, 2015, http://www.posiva.fi/files/4030/POSIVA_2015-01.pdf.

[16] T. Ahrens, *Rock Physics & Phase Relations*, AGU Reference Shelf, 1995.

[17] N. Bouhsane and S. Bouhlassa, "Assessing magnetic susceptibility profiles of topsoils under different occupations," *International Journal of Geophysics.*, vol. 2018, pp. 1–8, 2018, Article ID 9481405.

[18] F. Hrouda, "Models of frequency-dependent susceptibility of rocks and soils revisited and broadened," *Geophysical Journal International*, vol. 187, no. 3, pp. 1259–1269, 2011.

[19] M. Lehtinen, P. Nurmi, and T. Rämö, "3000 vuosimiljoonaa Suomen kallioperää," *Suomen Geologinen Seura*, 1998, Edition 1, Chapter 5.

[20] "Content page (ubc.ca)," https://www.eoas.ubc.ca/courses/eosc350/courses/eosc350/content/foundations/properties/magsuscept.htm.

[21] T. Alapieti and A. Kärki, "Field trip guidebook early Palaeoproterozoic (2.5-2.4) Tornio – Näränkävaara layered intrusion belt and related chrome and platinum-group element mineralization, northern Finland," in *The 10th Platinum Symposium in Oulu*, Geological Survey of Finland, Finland, 2005.

[22] I. Aaltonen, E. Heikkinen, S. Paulamäki, H. Säävuori, S. Vuoriainen, and I. Öhman, "Summary of petrophysical analysis of olkiluoto core samples 1990-2008," *Working Report 2009-11*, Posiva Oy, Eurajoki, 2009, http://www.posiva.fi/files/983/WR_2009-11_web.pdf.

[23] J. Schön, "Physical properties of rocks: fundamentals and principles of petrophysics," in *Handbook of Geophysical Exploration. Seismic Exploration*, K. Helbig and S. Treitel, Eds., vol. 18, p. 583, Oxford, OX, UK, 1996, Imprint.

[24] J. Mattila, "A system of nomenclature for rocks in olkiluoto," *Working Report 2006-32*, Posiva Oy, Eurajoki, 2006, http://www.posiva.fi/files/239/WR2006-32web.pdf.

[25] M. Silvast and B. Wiljanen, "Onkalo edz-measurements using ground penetrating radar (gpr) method," *Working Report 2008-58*, Posiva Oy, Eurajoki, 2008, http://www.posiva.fi/files/793/WR2008-58web.pdf.

[26] K. Khrustalev, R. Plenteda, C. Ames, I. Tsvetkov, and J. Emmer, "W.-S. Park Investigations of novel technologies for safeguarding geological repositories," International Atomic Energy Agency (IAEA), Vienna, Austria, 2020.